文章编号：0258-8013 (2009) 32-0058-08 中图分类号：TK 124 文献标志码：A 学科分类号：470·10

层流区 CuO–水纳米流体流动与对流换热特性

张邵波，骆仲泱，寿春晖，倪明江，岑可法

(能源清洁利用国家重点实验室(浙江大学)，浙江省 杭州市 310027)

Heat Transfer Properties of CuO-water Nanofluids in Laminar Flow

ZHANG Shao-bo, LUO Zhong-yang, SHOU Chun-hui, NI Ming-jiang, CEN Ke-fa

(State Key Laboratory of Clean Energy Utilization (Zhejiang University), Hangzhou 310027, Zhejiang Province, China)

ABSTRACT: The laminar convective heat transfer behavior of CuO nanoparticle dispersions in water with three different particle sizes (23, 51, and 76 nm) was investigated experimentally in a flow loop with constant heat flux. The main purpose of this study is to evaluate the effect of particle size on convective heat transfer in laminar region. The experimental results show that the suspended nanoparticles remarkably increase the convective heat transfer coefficient of the base fluid, and the nanofluid with 23 nm particles shows higher heat transfer coefficient than nanofluids containing the other two particle sizes about 10% under the same *Re*. Based on the effective medium approximation and the fractal theory, the effective thermal conductivity of suspension was obtained. It is shown that if the new effective thermal conductivity correlation of the nanofluids is used in calculating the Prandtl (*Pr*) and Nusselt number (*Nu*), the new correlation accurately reproduce the convective heat transfer behavior in tubes.

KEY WORDS: nanofluid; convective heat transfer coefficient; laminar flow; viscosity

摘要：测量了 3 种不同粒径(23、51 和 76 nm)的CuO –水纳米流体在层流状态下的管流对流换热系数，对比不同纳米颗粒粒径对层流区对流换热的影响。实验结果表明，在液体中添加纳米粒子增大了液体的管内对流换热系数，且在相同雷诺数条件下，23 nm粒径的纳米流体对流换热系数要比其他 2 种粒径的纳米流体对流换热系数高出大约 10%。基于有效介质理论和分型理论，得出新的纳米流体有效导热系数关联式，使用此关联式计算对流换热系数能够得到更加精确的实验方程。

关键词：纳米流体；对流换热系数；层流；黏度

基金项目：国家自然科学基金项目(50676082)。

Project Supported by National Natural Science Foundation of China (50676082).

0 INTRODUCTION

In recent years, due to the development of microelectromechanical systems (MEMS) and nanoelectromechanical systems (NEMS), enormous innovation for heat transfer enhancement is required. It has been proposed that nanometer-sized particles could be suspended in industrial heat transfer fluids such as water, ethylene glycol and oil to produce a new class of engineered fluids with high thermal conductivity [1]. Because of excellent thermal conductivity, nanofluid dispersions are important for a number of industrial sectors including transportation, power generation, micro-manufacturing and miniature devices in which sizes of components and flow passages are small [2-3].

Heat transfer tests have been conducted to assess thermal performance of oxide and metallic nanofluids under laminar flow conditions. Wen and Ding [4] published a study on an Al_2O_3/water nanofluid heat transfer under conditions of laminar flow at the tube entrance region under constant wall heat flux. The experiments were conducted for fluids that falls within the following: $600<Re<2200$. The results illustrated that local heat transfer coefficient varied with volume fraction and Reynolds number (*Re*). They claimed that the thermal developing length for this nanofluid was greater than that of pure water. The reason that heat transfer enhancement in enhanced with nanofluids is the decreased thermal boundary layer thickness due to the non-uniform distribution of thermal conductivity and viscosity, which results from

the Brownian motion of the nanoparticles. The convective heat transfer coefficients in the laminar flow region (*Re* = 5~110) of graphite nanofluids were measured by Yang et al [5]. The measurements demonstrated that the heat transfer coefficient increased with increasing *Re* and particle concentration. Recently, Xuan et al. [6-7] constructed an apparatus to investigate the convective heat transfer coefficient and friction factor of a Cu-water nanofluid in both laminar and turbulent flow regime. In their study of laminar flow in the range of *Re* between 800 and 2,300, the results showed that a small amount (i.e., less than 2%) of copper nanoparticles in deionized water remarkably improved the convective heat transfer. For example, the *Nu* for water containing 2.0 % of Cu nanoparticles was improved by more than 60% as compared to that of water. Furthermore, the *Nu* of the Cu/water dispersion increased with increasing particle volume fraction and *Re*. The Dittus-Boelter correlation failed to predict the improved experimental heat transfer behavior of the nanofluids. Xuan and Roetzel [8] considered two approaches to illustrate the heat transfer enhancement achieved by nanofluids. The first approach was to utilize the single phase model in which both the fluid phase and the particles are in thermal equilibrium state and flow at the same velocity. In the second analysis, they adopted the dispersion model to interpret nanofluids heat transfer enhancement resulting from the chaotic movement of nanoparticles in the main flow.

From the studies reviewed previously, few researches have reported on convective heat transfer with varying particle sizes. This paper is intended to experimentally study the convective heat transfer characteristics of CuO nanofluids of varying particle sizes. A more powerful microfluidic method was used to disperse nanoparticles into the base fluid. Furthermore, the results from calculation of several Nusselt correlations were compared with the measured data.

1　MATERIAL PREPARATION AND EXPERIMENTAL SYSTEM

1.1　Material preparations

Nanoparticles of CuO with an equivalent spherical diameter (ESD) of 51nm and 76 nm were obtained from NanoProducts Corporation; nanoparticles of CuO with an ESD of 23 nm were obtained from Afla Aesar Corporation. The powders were dispersed into deionized (DI) water and fully blended in a blender. Then, a microfluidic process system that can produce 500mL of nanofluid per hour was employed to further disperse and deagglomerate the particles. This system contains an air-powered intensifier pump, which is designed to supply a constant rate of the desired pressure to the dispersion stream. As the pump travels through its pressure stroke, it drives the dispersion at a constant pressure in the range of 200 to 1 600 atmospheric pressures through precisely defined fixed-geometry micro-channels within the interaction chamber. As a result, the dispersion stream accelerates to high velocities, thereby creating shear rates within the stream that are orders of magnitude greater than those created by any other conventional means. This system can achieve better results in terms of uniform particle and droplet size reduction, deagglomeration, and high-yield cell disruption. In order to obtain uniformity and a satisfactory dispersible suspension, we used sodium dodecyl-benzenesulfonate (SDBS) as a dispersant. In our experiment, 1% SDBS was added into a 1% CuO-water nanofluid, which was produced by microfluidic process system, under the condition of supersonic vibration. Then hydrochloric acid or sodium hydroxide was added to adjust the pH value of the dispersed fluid. When the pH value was approximately 8, the absolute value of the zata-potential was the largest; and the particle size was the smallest; and the nanofluid was the most stable. The dispersed fluid was allowed to settle for one week.

Figure 1 shows the typical micrographs obtained by transmission electron microscopy (TEM) for the CuO nanoparticles that were used in this study. The figures (a), (b), and (c) confirm that the average size as specified by the manufacturers was in the range of 23, 51, and 76 nm, respectively.

1.2　Thermal conductivity and viscosity

The effective thermal conductivity of the nanofluid was measured with a KD Ⅱ thermal property

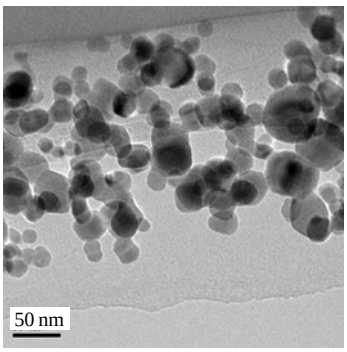

(a) 23 nm

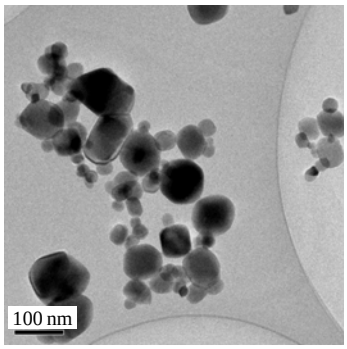

(b) 51 nm

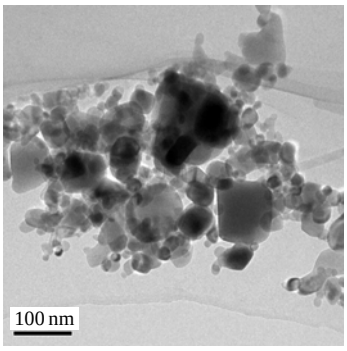

(c) 76 nm

图 1 CuO 纳米颗粒透射电镜照片

Fig. 1 Typical TEM micrographs of CuO nanoparticles

meter (Labcell Ltd, UK), which operates using a method based on the transient hot wire method. The uncertainty of the measurements is within 3% under the conditions of liquid measurement [3]. A typical set of results are shown in Figure 2 for measurements at 20 ℃. The effective thermal conductivity of the nanofluid increases approximately linearly with particle volume fraction but decreases with increasing particle sizes [9-10]. The thermal conductivity variations at different temperatures of the nanofluids were also measured, and the corresponding values were used for the evaluation of *Nu* in the convective heat transfer analysis due to the well known temperature effect on nanofluid conductivity.

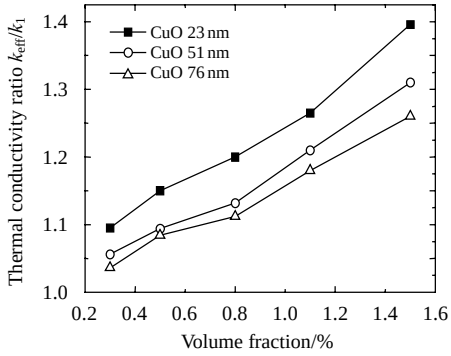

图 2 纳米流体导热系数

Fig. 2 Thermal conductivity of sample fluids

The viscosity of the suspensions was determined with an Ubbelohde-type (Schott-Gerate) capillary viscometer for dilution. The capillary viscometer was calibrated using DI water at 20, 30, 40, and 50 ℃ to determine the constants of the apparatus. The kinematic viscosity results are shown in Figure 3 and are used for the calculation of convective heat transfer. Einstein's theory [11] seems to predict the viscosities for nanofluids generally correctly.

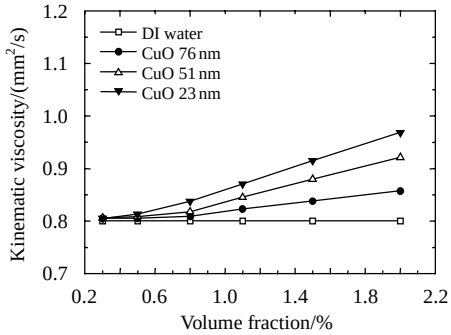

图 3 纳米流体黏度

Fig. 3 Kinematic viscosity of sample fluids

Thus, Einstein's equation is as follow:

$$\mu_{nf} = \mu_w(1+2.5\phi) \quad (1)$$

Where μ_{nf} is the nanofluid viscosity, μ_w is the base fluid viscosity, and φ is the nanoparticle volume fraction. This equation is valid for dilute suspensions of spherical particles and may be used with confidence for nanofluids with larger particle sizes.

1.3 Convective experimental setup

Figure 4 shows the experimental apparatus for the investigation of the flow and convective heat transfer characteristics of water-based CuO nanofluid flowing through a circular tube with a constant heat flux under turbulent flow conditions. The experimental

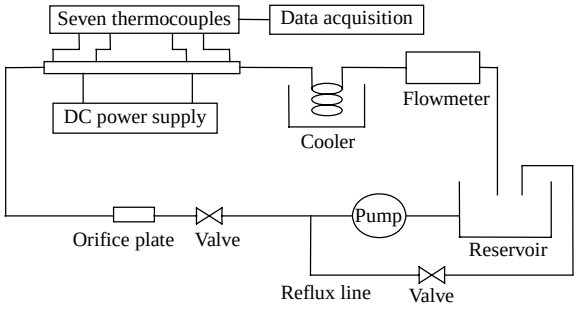

图 4　对流换热实验系统

Fig. 4　Heat transfer testing apparatus

system mainly consisted of a closed flow loop, a heating unit, a cooler, and a measuring and controlling unit. The flow loop included a pump, a digital flowmeter, a 6 liter reservoir, and a test section. The reservoir tank was made of polymethylmethacrylate and was intended to hold the nanofluid and to monitor the dispersion behavior and the stability of the nanofluid. In order to control the fluid flow rate, a reflux line with a valve was used. The cooler was used to keep a constant temperature for the dispersion at the inlet of the test section. A digital flowmeter with 5% precision was setup with two adjusting valves, i.e., one at the main flow loop and the other at the by-pass line. The straight copper tube with an inner diameter of 10 mm and a length of 900 mm was used as the test section. The tube surface was electrically heated by a DC power supply with a maximum power of 3 kW to generate constant heat flux. Additionally, it was thermally insulated with a 150 mm thick blanket to minimize the heat loss from the tube to the ambient air. Five T-type thermocouples were brazed on the outer wall at the axial positions of the heat transfer test section to measure the wall temperatures, whereas the other two T-type thermocouples were located at the inlet and exit of the test section to measure the bulk temperatures of the fluid. To preserve a constant temperature at the inlet of the test section, the heated fluid returns to the reservoir tank after passing through a cooler.

After injection of the nanofluid of a specified concentration in the reservoir tank, the pump and cooling systems were started. The flow rate was regulated by using the valve on the reflux line, and the tests were repeated for at least ten flow rates with each concentration. During experimental runs, the inlet and outlet temperatures of the nanofluid, the tube wall temperature at different positions and the flow rate were measured. Each measurement was repeated at least twice, and the flow system was cleaned between runs, even for those runs using the same material, to prevent fouling on the inner tube wall and the thermocouple heads.

2　EXPERIMENTAL RESULTS AND DISCUSSION

2.1　Problem formulation

The nanofluid convective heat transfer coefficient (h_{nf}) and the Nu_{nf} are calculated as follows:

$$h_{\mathrm{nf}}(\exp)=\frac{C_{p\mathrm{nf}}\rho_{\mathrm{nf}}UA(T_{\mathrm{b2}}-T_{\mathrm{b1}})}{\pi DL(T_{\mathrm{w}}-T_{\mathrm{b}})} \tag{2}$$

$$Nu_{\mathrm{nf}}(\exp)=\frac{h_{\mathrm{nf}}D}{k_{\mathrm{nf}}} \tag{3}$$

Where $C_{p\mathrm{nf}}$ is the specific heat of nanofluid, ρ_{nf} is the density of nanofluid, U is the average fluid velocity, A is the tube cross section area, D is the diameter of test tube, L is the length of test tube, T_{b1} is the inlet bulk temperature of nanofluid, T_{b2} is the exit bulk temperature of nanofluid, T_{b} is the average bulk temperature of nanofluid, T_{w} is the tube wall temperature, and k_{nf} is the thermal conductivity of nanofluid.

The correlation as proposed by Yu and Choi [12] was used to determine the nanofluid effective thermal conductivity as follows:

$$k_{\mathrm{nf}}=\left[\frac{k_{\mathrm{s}}+2k_{\mathrm{f}}+2(k_{\mathrm{s}}-k_{\mathrm{f}})(1+\beta)^{3}\phi}{k_{\mathrm{s}}+2k_{\mathrm{f}}-(k_{\mathrm{s}}-k_{\mathrm{f}})(1+\beta)^{3}\phi}\right]k_{\mathrm{f}} \tag{4}$$

In Equation 4 β is the ratio of the nanolayer thickness to the original particle radius, k_{s} is the thermal conductivity of solid particle, k_{f} is the thermal conductivity of base fluid. This correlation points out that the solid/liquid interfacial layers play an important role in the enhanced thermal conductivity of nanofluids [13-14].

Wang [15] reported that a nanoparticle suspension is composed of a host liquid and percolation patterned cluster inclusions. The lognormal distribution function could be used to describe the spatial distribution of an isolated cluster, $n(r)$ [16].

$$n(r)=\frac{1}{r\sqrt{2\pi}\ln\sigma}\exp\{-[\frac{\ln(r/\bar{r})}{\sqrt{2}\ln\sigma}]^2\} \quad (5)$$

Where $\bar{r}$ is the geometric mean radius, and σ is the standard deviation. Considering the effect of particle clustering and cluster distribution, they obtained the effective thermal conductivity of suspension using the following equation:

$$\frac{k_{\mathrm{nf}}}{k_{\mathrm{f}}}=\frac{(1-\phi)+3\phi\int_0^{\infty}\frac{k_{\mathrm{cl}}(r)n(r)}{k_{\mathrm{cl}}(r)+2k_{\mathrm{f}}}\mathrm{d}r}{(1-\phi)+3\phi\int_0^{\infty}\frac{k_{\mathrm{f}}n(r)}{k_{\mathrm{cl}}(r)+2k_{\mathrm{f}}}\mathrm{d}r} \quad (6)$$

Using the multi-component MG model as proposed by Wood and Ashcroft [17], we can obtained the effective thermal conductivity of a suspension with overall consideration of cluster distribution and the surface adsorption of nanoparticles. By substituting the effective thermal conductivity of clusters, $k_{\mathrm{nf}}(r)$, and the radius distribution function, $n(r)$, into the MG equation, the effective thermal conductivity of a nanoparticle suspension (k_{pnf}) can be expressed as:

$$\frac{k_{\mathrm{pnf}}}{k_{\mathrm{f}}}=\frac{1+2\phi\int_0^{\infty}\frac{(k_{\mathrm{nf}}(r)-k_{\mathrm{f}})n(r)(1+\beta)^3}{k_{\mathrm{s}}(r)+2k_{\mathrm{f}}}\mathrm{d}r}{1-\phi\int_0^{\infty}\frac{(k_{\mathrm{nf}}(r)-k_{\mathrm{f}})n(r)(1+\beta)^3}{k_{\mathrm{nf}}(r)+2k_{\mathrm{f}}}\mathrm{d}r} \quad (7)$$

The rheological and physical properties of the nanofluid were calculated at the mean temperature. Then, the *Nu* and convective heat transfer coefficients at different concentrations were calculated. The uncertainty in the measurement of thermal conductivity and viscosity was less than 3% and 0.5%, respectively. The systematic uncertainty analysis was carried out for derived quantities, and the maximum error in the *Re* and *Nu* values were evaluated at approximately 3% and 2%, respectively.

2.2 Calibration of experimental system

In the heat transfer experiments, the voltage and current from the power supply were recorded, and the temperature readings from the seven thermocouples were registered using a data acquisition system. The thermocouples were calibrated in a thermostatically controlled water bath. We conducted a pilot experiment with water as the fluid to estimate the reliability and accuracy of the entire experimental system. The results of the pilot experiment are compared with the calculated values obtained with the well-known Seider-Tate equation [18].

$$Nu_{\mathrm{nf}}=1.86Pe_{\mathrm{nf}}^{1/3}(\frac{D}{L})^{1/3}(\frac{\mu_{\mathrm{nf}}}{\mu_{\mathrm{wnf}}})^{0.14} \quad (8)$$

Where Pe_{nf} is the Peclet number of nanofluid, and μ_{wnf} is the nanofluid viscosity at tube wall temperature.

As shown in Figure 5, the good conformity between the experimental results and the calculated values for water validates the precision of the experimental system. The uncertainty of the experimental system is within 10%.

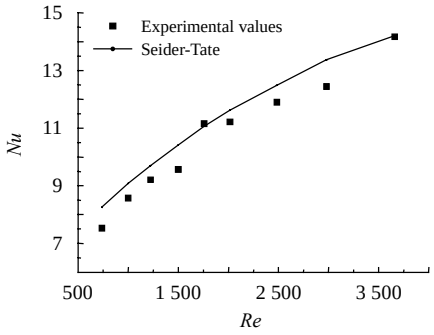

图 5 去离子水对流换热实验值与 Seider-Tate 方程理论值对比

Fig. 5 Comparison between *Nu* of experimental investigation and Seider–Tate equation for distilled water

2.3 Experimental results

Experiments for nanofluids were performed over a range of *Re,* i.e., 650-2450, and for various concentrations of CuO nanofluids (0.3%~1.5%). The results are presented and discussed in this section.

Figure 6 (a) illustrates the tendency for variation in the *Nu* of the dispersion with different *Re* of nanofluids with the 23 nm particle size at various particle concentrations. This demonstrates the effect of nanoparticle concentration. The experimental results indicate that the suspended nanoparticles remarkably improve the heat transfer performance of the base fluid. As compared to water, the maximum increase for the *Nu* is about 30 percent for the dispersion with a volume fraction of 1.5% of nanoparticles. The experimental results also indicate that the heat transfer feature of a nanofluid remarkably increases with the volume fraction of nanoparticles. The particle volume fraction is one of the main factors that affect the *Nu* of the nanofluid. For example, while

the volume fraction of the nanoparticles increased from 0.3% to 1.5% the increase in the *Nu* of the dispersion compared with that of water varied from 8% to 30% for the same *Re* conditions. Figure 6(b) and Figure 6(c) represent the results for 51 and 76 nm particles, respectively. The tendency of the *Nu* to increase with increasing volume fraction for the 51 nm and 76 nm nanofluids is similar to that of the 23nm nanofluid. The figures show that although the trend is similar to the nanofluid with the small particle size, the magnitude of enhancement is lower than for that of the nanofluid with the smaller particles.

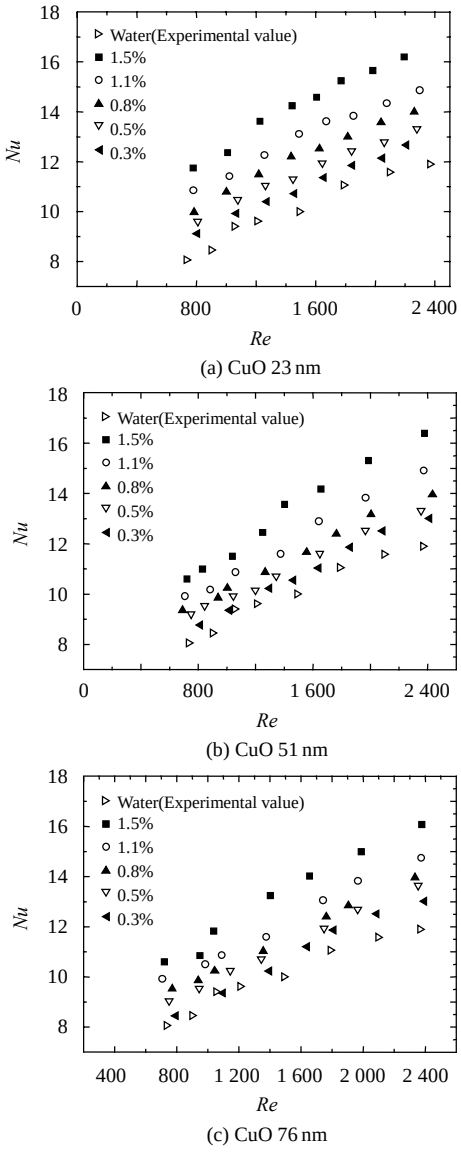

图 6　*Nu* 随 *Re* 的变化

Fig. 6　Variation of *Nu* with *Re* number

Nanofluids with 23 nm particles demonstrate a greater enhancement in heat transfer coefficient than the nanofluids containing the other two particle sizes and water. In order to determine whether the increase in the heat transfer coefficient is due to the increase in thermal conductivity or other thermophysical properties, non-dimensional heat transfer coefficients are investigated. Figure 6 and Figure 7 show the non-dimensional heat transfer variation for 23, 51, and 76 nm nanofluids at 1.5% with varying *Re* numbers. Here the *Nu* is calculated based on the thermal conductivity values measured at that concentration, particle size, and average bulk fluid temperature. This plot implies that the increase in the heat transfer coefficient is much higher as compared to the increase in thermal conductivity. For a 23 nm nanofluid at an *Re* of 1800, the enhancement of the heat transfer coefficient is about 32%, whereas the thermal conductivity only increased only by 23%. Similarly for the 51 and 76 nm nanofluids, the enhancements of the heat transfer coefficients are about 24% and 22%, respectively, whereas the thermal conductivities increased by about 18% and 15%, respectively. Thus, it suggests that the convective heat transfer of nanofluids cannot be explained by the increase in thermal conductivity alone and may be explained by particle migration effects and thermal dispersion [19-20].

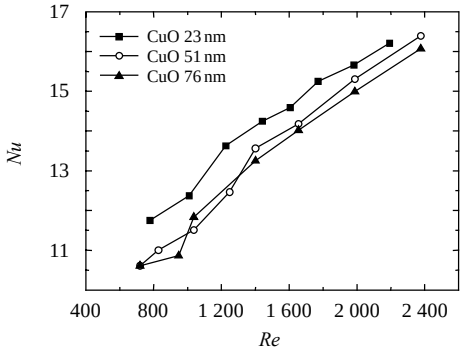

图 7　3 种粒径在体积份数为 1.5%时 *Nu* 的对比

Fig. 7　Comparisons of the three particle diameters at volume fraction of 1.5 %

The experimental results obtained from this investigation were compared with the prediction of the Seider-Tate equation [11]. In this correlation, nanofluid convective heat transfer enhancement is due to the thermal conductivity increase. A parity plot for the above correlation is shown in Figure 8. It shows

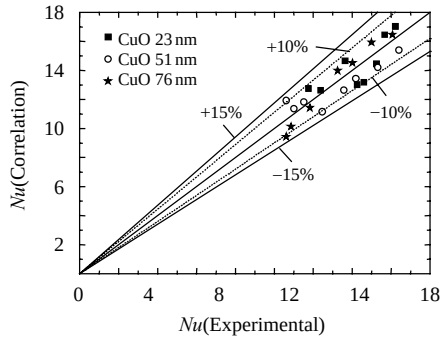

图 8 实验值与计算值对比

Fig. 8 Parity plot comparing the correlation and experimental results

that the correlation falls in the region of ±15% deviation. Please note that this correlation is a framework on which future correlations can be built over a wider range of parameters when experimental data becomes available.

3 CONCLUSIONS

The convective heat transfer features and flow performance of CuO-water nanofluids with three different particle sizes (23, 51, and 76 nm) in a tube have been investigated. Experiments for nanofluids were performed over a range of *Re,* i.e., 650-2 450, and for various concentrations of CuO nanofluids (0.3%~1.5 %).

The sample nanofluids used in this study show that the heat transfer performance of a nanofluid is better than the base fluid in terms of *Nu* with *Re*, and the convective heat transfer coefficient of the dispersion increases with the volume fraction of nanoparticles. Nanofluids with 23 nm particles demonstrate a greater enhancement in heat transfer coefficient than the nanofluids containing the other two particle sizes and water. For a 23 nm nanofluid at an *Re* of 1800, the enhancement of the heat transfer coefficient is about 32%, whereas the thermal conductivity only increased only by 23%.Similarly for the 51 nm and 76nm nanofluids, the enhancements of the heat transfer coefficients are about 24% and 22%, respectively, whereas the thermal conductivities increased by about 18% and 15%, respectively. Thus, it suggests that the convective heat transfer of nanofluids cannot be explained by the increase in thermal conductivity alone and may be explained by particle migration effects and thermal dispersion

Based on the effective medium approximation and the fractal theory, the article derives a new effective thermal conductivity for calculating the nanofluid convective heat transfer. The calculated result is quiet close to practical value when verified by experiment with error within ±15%.

REFERENCES

[1] Choi S，Siginer D，Wang H．Enhancing thermal conductivity of fluids with nanoparticles[J]．American Society of Mechanical Engineers Federal，1995，231(66)：99-103．

[2] 姚寿广，马哲树，陈如冰．一种新型结构的热管式散热冷板性能的数值模拟试验与分析[J]．中国电机工程学报，2005，25(7)：41-45．
Yao Shouguang，Ma Zheshu，Chen Lubin．Numerical experimental study and analysis of performance for heat pipe cooling flat-plate with a newly structure[J]．Proceedings of the CSEE，2005，25(7)：41-45(in Chinese)．

[3] 熊建国，刘振华．平板热管微槽道传热面上纳米流体沸腾换热特性[J]．中国电机工程学报，2007，27(23)：105-109．
Xiong Jianguo，Liu Zhenhua．Boiling heat transfer characteristics of nanofluids on flat heat pipe evaporator with micro-grooved surface[J]．Proceedings of the CSEE，2007，27(23)：105-109(in Chinese)．

[4] Wen D，Ding Y．Experimental investigation into convective heat transfer of nanofluids at the entrance region under laminar flow conditions[J]．International Journal of Heat and Mass Transfer，2004，47(24)：5181-5188．

[5] Yang Y，Zhang Z，Grulke E，et al．Heat transfer properties of nanoparticle-in-fluid dispersions (nanofluids) in laminar flow [J]．International Journal of Heat and Mass Transfer，2005，48(6)：1107-1116．

[6] Xuan Y，Li Q．Investigation on convective heat transfer and flow features of nanofluids[J]．Journal of Heat Transfer，2003，125(11)：151-155．

[7] Li Q，Xuan Y，Jiang J，Xu J．Experimental investigation on flow and convective heat transfer feature of a nanofluid for aerospace thermal management[J]．Journal of Astronautics，2005，26(4)：391-394．

[8] Xuan Y，Roetzel W．Conceptions for heat transfer correlation of nanofluids[J]．International Journal of Heat and Mass Transfer，2000，43(19)：3701-3707．

[9] Lee S，Choi S，Li S．Measuring thermal conductivity of fluids containing oxide nanoparticles[J]．ASME Journal of Heat Transfer，1999，2(121)：280-289．

[10] Xie H，Wang J，Xi T．Thermal conductivity enhancement of suspension containing nanosized alumiua particles[J]．Journal of Applied Physics，2002，91(7)：4568-4572．

[11] Einstein A．Investigations on the theory of the brownian movement [M]．New York：Dover Publications，1956：1-18．

[12] Yu W，Choi S．The role of international layers in the enhanced thermal

conductivity of nanofluids: a renovated Maxwell model[J]. Journal of Nanoparticle Research，2003，5(1-2)：167-171.

[13] Xue Q. Model for effective thermal conductivity of nanofluids [J]. Physics Letters A，2003，307(5-6)：313-317.

[14] Keblinski P，Phillpot S，Choi S U S. Mechanisms of heat flow in suspensions of nano-sized particles(nanofluids)[J] . International Journal of Heat and Mass Transfer，2002，45(4)：855-863.

[15] Wang B，Zhou L，Peng X. A fractal model for predicting the effective thermal conductivity of liquid with suspension of nanoparticles [J]. International Journal of Heat and Mass Transfer，2003， 46 (14)：2665-2672.

[16] Chylek P， Srivastava V. Dielectric constant of a composite inhomogeneous medium[J]. Physical Review B，1983，27(8)：5098-5106.

[17] Wood D，Ashcroft N. Effective medium theory of optical properties of small particle composites[J]. Philosophical Magazine，1977，35(2)：269-280.

[18] Seider E，Tate G. Heat transfer and pressure drop of liquid in tubes[J]. Industrial and Engineering Chemistry Research，1936，28(12)：1429-1435.

[19] Buongiorno J. Convective transport in nanofluids[J]. Journal of Heat Transfer，2006，128(3)：240-250.

[20] 过增元. 国际传热研究前沿—微细尺寸传热[J]. 力学进展，2000，30(1)：1-6.
Guo Zengyuan. Frontier of heat transfer—microscale heat transfer [J]. Advances in Mechanics，2000，30(1)：1-6.

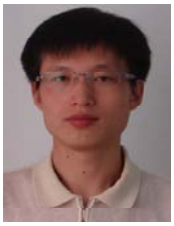
张邵波

收稿日期：2009-03-27。

作者简介：

张邵波(1977—)，男，博士研究生，研究方向为纳米流体热物理特性研究，zhang05@zju.edu.cn；

骆仲泱(1962—)，男，博士，教授，博士生导师，主要从事洁净煤燃烧及生物质利用研究；

岑可法(1935—)，男，博士，教授，中国工程院院士，主要从事能源清洁利用和污染控制技术研究。

(责任编辑　王庆霞)